Published in final edited form as:
Mol Cancer Ther. 2011 February ; 10(2): 360–371. doi:10.1158/1535-7163.MCT-10-0760.

Preclinical pharmacology, antitumor activity and development of pharmacodynamic markers for the novel, potent AKT inhibitor CCT128930

Timothy A. Yap[1,§], **Mike I. Walton**[1,§], **Lisa-Jane K. Hunter**[1], **Melanie Valenti**[1], **Alexis de Haven Brandon**[1], **Paul D. Eve**[1], **Ruth Ruddle**[1], **Simon P. Heaton**[1], **Alan Henley**[1], **Lisa Pickard**[1], **Gowri Vijayaraghavan**[1], **John J. Caldwell**[1], **Neil T. Thompson**[2], **Wynne Aherne**[1], **Florence I. Raynaud**[1], **Suzanne A. Eccles**[1], **Paul Workman**[1], **Ian Collins**[1], and **Michelle D. Garrett**[1,*]

[1]Cancer Research UK Cancer Therapeutics Unit, The Institute of Cancer Research, 15 Cotswold Road, Sutton, Surrey SM2 5NG, UK

[2]Astex Therapeutics, 436 Cambridge Science Park, Cambridge CB4 0QA, UK

Abstract

AKT is frequently deregulated in cancer, making it an attractive anticancer drug target. CCT128930 is a novel ATP-competitive AKT inhibitor discovered using fragment and structure-based approaches. It is a potent, advanced lead pyrrolopyrimidine compound exhibiting selectivity for AKT over PKA, achieved by targeting a single amino acid difference. CCT128930 exhibited marked antiproliferative activity and inhibited the phosphorylation of a range of AKT substrates in multiple tumor cell lines *in vitro*, consistent with AKT inhibition. CCT128930 caused a G1 arrest in *PTEN*-null U87MG human glioblastoma cells, consistent with AKT pathway blockade. Pharmacokinetic studies established that potentially active concentrations of CCT128930 could be achieved in human tumor xenografts. Furthermore, CCT128930 also blocked the phosphorylation of several downstream AKT biomarkers in U87MG tumor xenografts, indicating AKT inhibition *in vivo*. Antitumor activity was observed with CCT128930 in U87MG and HER2-positive,

[*]**Corresponding Author** Michelle D. Garrett, Ph.D. Cancer Research UK Cancer Therapeutics Unit, The Institute of Cancer Research, 15 Cotswold Road, Sutton, Surrey SM2 5NG, United Kingdom. Tel: +44-20-8722-4352 Fax: +44-20-8722-4126 michelle.garrett@icr.ac.uk.
[§]Joint first authors

Financial Support
Grant support was provided to TAY, MIW, LJKH, MV, AdHB, PDE, RR, AH, LP, GV, JJC, FIR, SAE and MDG by Cancer Research UK (CR-UK) grant number C309/A8274, to SPH by CR-UK grant number C51/A6883, to PW by CR-UK grant number C309/A8992 and to WA and IC by CR-UK grant number C309/8365. Additional support was provided to SAE and MDG by The Institute of Cancer Research and to LJKH by Astex Therapeutics. This work was carried out as part of a funded research collaboration with Astex Therapeutics. We acknowledge NHS funding to the NIHR Biomedical Research Centre.

Potential Conflicts of Interest
Timothy A Yap, Mike I. Walton, Lisa-Jane K. Hunter, Melanie Valenti, Alexis de Haven Brandon, Paul Eve, Ruth Ruddle, Simon P. Heaton, Alan Henley, Lisa Pickard, Gowri Vijayaraghavan, John J. Caldwell, Wynne Aherne, Florence I. Raynaud, Suzanne A. Eccles, Paul Workman, Ian Collins and Michelle D. Garrett are current or former employees of The Institute of Cancer Research, which has a commercial interest in the development of AKT inhibitors, including CCT128930, and operates a rewards for inventors scheme. Neil T. Thompson is an employee of Astex Therapeutics, which also has a commercial interest in the development of AKT inhibitors including CCT128930. Both Astex Therapeutics and The Institute of Cancer Research have been involved in a commercial collaboration with Cancer Research Technology Limited (CRT) to discover and develop inhibitors of AKT and intellectual property arising from this program has been licensed to AstraZeneca.

Europe PMC Funders Author Manuscripts

PIK3CA-mutant BT474 human breast cancer xenografts, consistent with its pharmacokinetic and pharmacodynamic properties. A quantitative immunofluorescence assay to measure the phosphorylation and total protein expression of the AKT substrate PRAS40 in hair follicles is presented. Significant decreases in pThr246 PRAS40 occurred in CCT128930-treated mouse whisker follicles *in vivo* and human hair follicles treated *ex vivo*, with minimal changes in total PRAS40. In conclusion, CCT128930 is a novel, selective and potent AKT inhibitor, which blocks AKT activity *in vitro* and *in vivo* and induces marked antitumor responses. We have also developed a novel biomarker assay for the inhibition of AKT in human hair follicles, which is currently being employed in clinical trials.

Keywords

CCT128930; AKT inhibitor; preclinical pharmacology; antitumor activity; hair follicles

Introduction

The serine-threonine kinase AKT (protein kinase B) is a key component of the phosphatidylinositol 3-kinase (PI3K)-AKT-mammalian target of rapamycin (mTOR) signaling network, with activation resulting in increased cell survival, proliferation, and growth (1, 2). AKT is activated following the binding of its pleckstrin homology (PH) domain with cell membrane phosphatidylinositol (3,4,5)-trisphosphate (PIP_3), which is produced by PI3K (3). This leads to the phosphorylation of AKT residues threonine 308 by phosphoinositide-dependent kinase 1 (PDK1) (4), and serine 473 by the mammalian target of rapamycin complex 2 (mTORC2) (5). Activated AKT results in phosphorylation of important downstream proteins involved with cell proliferation, survival and growth, such as glycogen synthase kinase-3β (GSK3β) (6), the forkhead family of transcription factors (7), proline-rich AKT substrate 40 (PRAS40) and S6 ribosomal protein (S6RP) (8).

Hyperactivation of the PI3K-AKT-mTOR signaling network is involved in malignant transformation and chemoresistance, and may occur through upstream stimulation by receptor tyrosine kinases or genetic abnormalities of key pathway components, such as the tumor suppressor *PTEN* (phosphatase and tensin homolog on chromosome 10), *PIK3CA* and *AKT* (1, 9). The promising clinical activity observed with agents targeting the mTOR kinase has shown that targeting the PI3K-AKT-mTOR pathway is a rational and effective anticancer approach (10). AKT thus represents an attractive target for the development of anticancer agents (2).

We have used fragment-based *in silico* screening to identify hits against AKT, which were subsequently validated through structural studies, and transformed into potent lead compounds using structure-based design (11, 12). As a result of these endeavors, CCT128930, a potent small molecule inhibitor of AKT with drug-like properties was discovered from a series of pyrrolopyrimidines (12). Importantly, CCT128930 demonstrates selectivity for AKT over PKA by targeting a single amino acid difference, which we were the first to show (12, 13). Hence this was an important compound to profile in model systems and to use as a chemical probe (14).

Europe PMC Funders Author Manuscripts

The development of selective, molecularly targeted therapeutics requires the identification of biologically active concentrations through pharmacokinetic profiling to demonstrate appropriate drug exposures and pharmacodynamic measurements that confirm target and pathway modulation *in vivo*. Such a demonstration of a pharmacologic audit trail necessitates the development and validation of appropriate pharmacodynamic biomarkers (15–17). While pharmacodynamic biomarker responses in tumors are the most relevant indicator of target modulation, issues of accessibility mean that surrogate normal tissues are frequently employed. Since the bulbs of hair follicles contain rapidly proliferating cells and sampling is both accessible and minimally invasive, plucked hairs are potentially suitable tumor surrogates for serial pharmacodynamic analyses. Previous studies have shown that hair follicles may be used to monitor the pharmacodynamic effects of PI3K inhibitors, and this format may potentially be readily integrated into early clinical trials (18, 19).

In this paper, we present the preclinical pharmacology of the novel AKT inhibitor CCT128930 and demonstrate its effects on appropriate pharmacodynamic biomarkers, both *in vitro* and *in vivo*, as well as promising antitumor efficacy in human tumor xenograft models with PI3K-AKT-mTOR pathway activation. Using CCT128930 as a preclinical tool, we have also developed a robust and sensitive, non-invasive pharmacodynamic biomarker assay using hair follicles, which is currently being employed in a clinical trial of an AKT inhibitor (20).

Materials and Methods

Cell Culture and Reagents

All cell lines were purchased from the American Type Culture Collection (Rockville, MD, USA) and grown in their recommended culture medium, supplemented with 10% fetal bovine serum at 37°C in 5% CO_2 and passaged for less than six months prior to replacement from early passage frozen stocks. CCT128930 (12) and LY294002 (Calbiochem, Merck Biosciences) were made up as 10mM stocks in dimethyl sulphoxide (DMSO). All other reagents were purchased from Sigma (Poole, Dorset, UK) unless otherwise stated. Cells were regularly screened for *Mycoplasma* using a PCR-based assay (VenorGem, Minerva Biolabs).

Kinase Assays

Profiling against 50 different human kinases was carried out using 10 μmol/L CCT128930 at an ATP concentration equivalent to the Km for each enzyme (Millipore). All other enzyme assays were performed at Millipore (Dundee, UK).

Antiproliferative Assays

Cells were seeded in 96-well plates and allowed to attach for 36 hours to ensure exponential growth prior to treatment. *In vitro* antiproliferative activity was determined using a 96-hour SRB assay, and GI_{50} values were derived as described previously (21).

Protein Immunoblotting

Drug-treated cells were washed with ice-cold phosphate buffered saline, harvested, lysates prepared and protein estimations performed as described previously (22). Samples were separated on precast 10% Tris-glycine gels (Novex, Invitrogen) and transferred to polyvinylidene difluoride membrane (Millipore). The membranes were blocked for 1 hour in a blocking buffer (5% dried milk in 50 mmol/L Tris (pH 8.0), 150 mmol/L NaCl and 0.1% Tween 20), before incubating overnight at 4°C, in the following antibodies diluted in blocking buffer: AKT, phospho-AKT (Ser473), phospho-GSK3β (Ser9), phospho-S6RP (Ser240/244), S6RP, FOXO1, PRAS40, all at 1:1000, phospho-S6RP (Ser235/236) at 1:10,000, phospho-FOXO1 (Thr24)/FOX3a (Thr32) at 1:500 (all purchased from Cell Signaling Technology), phospho-PRAS40 (Thr246), p21 and p27 at 1:1000 (Upstate Biotechnology), GSK3β at 1:1000 (BD Biosciences, Oxford, UK), cyclin D1 Ab-1 (DCS-6) at 1:1000 (NeoMarkers, Lab Vision, Freemont, CA, USA) and glyceraldhyde-3-phosphate dehydrogenase at $1:1\times10^6$(Chemicon International, Millipore). The membranes were washed before incubation in goat anti-rabbit (1:5000 or 1:10000) or anti-mouse (1:10,000) HRP-conjugated secondary antibody (Bio-Rad) for 1 hour at room temperature. Protein bands were visualized with enhanced chemiluminescence reagents (Pierce, Thermo Fisher) on Hyperfilm (GE Healthcare) using a Compact X4 developer (Xograft).

Flow Cytometry

PTEN-null U87MG human glioblastoma cells were treated with CCT128930 and labeled with bromodeoxyuridine (BrdUrd) and propidium iodide (PI) (23), before being analyzed as previously described (22).

In vivo Human Tumor Xenograft Studies

All procedures were performed in accordance with National Home Office regulations under the Animals (Scientific Procedures) Act 1986 and within guidelines set out by the Institute's Animal Ethics Committee and by the UKCCCR and UK NCRI (24). *PTEN*-null U87MG human glioblastoma cells (2×10^6) were injected subcutaneously (s.c.) in the right flank of 6-8 weeks old female CrTacNCr-*Fox1nu* mice. For HER2-positive, *PIK3CA*-mutant BT474 human breast cancer xenografts, cells (5×10^6) were administered s.c. in medium supplemented with matrigel (1:1) into the mammary fat pads of female mice implanted s.c. with estradiol pellets (0.025 mg, 90 day release #NE-121, Innovative Research of America) 3 days previously. Animals were randomized and treatment was started with vehicle or CCT128930 when established tumors were ~100 mm^3 in mean volume. Control mice received vehicle only (10% DMSO, 5% Tween 20, 85% saline) and treated mice received 50 mg/kg CCT128930 intraperitoneally (i.p.) daily for 5 days (U87MG human glioblastoma xenografts) or 40 mg/kg CCT128930 i.p. twice daily for 5 days (BT474 human breast cancer xenografts). Tumor size and body weight were monitored three times a week. Tumor size was evaluated by measurement of 2 orthogonal diameters with calipers and volume was calculated from the formula: $V= 4/3\pi[(d1+d2)/4]^3$. At the end of the study, tumors were excised and weighed.

To assess the pharmacokinetic and pharmacodynamic profiles of CCT128930, a single dose of compound (50 mg/kg i.p.) was administered to mice bearing U87MG human

glioblastoma xenografts. Plasma and tumor samples were harvested at 2 and 6 hours following dosing. Mice were bled by cardiac puncture and plasma samples were collected and frozen at −20°C until analysis. Tumors were dissected, divided into two approximately equal pieces and snap frozen in liquid nitrogen until analysis. For pharmacodynamic studies, tumors were homogenized using a buffer containing 50 mmol/L Tris (pH 7.4), 1 mmol/L NaCl, 1 mmol/L EDTA, 1% Triton X-100, 1 mmol/L NaF, 1 mmol/L $NaVO_4$, 5 μmol/L Fenvalerate, 5 μmol/L Vbphen, 10 mg/mL TLCK, 1× Complete inhibitor tablet per 10-mL buffer (Roche), protease inhibitor cocktail, and phosphatase inhibitor 1 and 2 (Sigma-Aldrich) (25). Protein content was measured using Bradford reagent (26) and samples were analyzed using immunoblotting as described above.

Pharmacokinetic Analysis

Concentrations of CCT128930 in biological samples were determined using LC-MS. Drug was extracted using methanol and chromatography carried out on a Synergi-Polar RP column (5.0 cm × 4.6 mm ID, 4 μm particle size, Phenomenex, Macclesfield, UK) using a Waters 600MS pump and a 717 autosampler (Waters, Elstree, UK) with a gradient mobile phase of 0.1% formic acid/methanol at 0.6ml/min over 12 minutes. Detection was by LC-MS using a TSQ700 triple quadrapole in which the analyte was ionized by electrospray interface in positive mode to monitor the transition $[M+H]^+$ 342.8 to 146.6.4. The spray voltage was optimized to 5.5Kv and capillary temperature to 260ºC. The assay was linear over the range 10 – 10,000 nM CCT128930.

PRAS40 Immunofluorescence Studies

U87MG human glioblastoma cells were plated at 5×10^4 cells/well on cover slips in 24-well plates for 36 hours, before being treated with increasing concentrations of CCT128930 for 24 hours. Cells were fixed in 3.8% formaldehyde and permeabilized with 0.01% Triton X-100. BALB/c mice were treated with 50 mg/kg CCT128930 i.p. daily for 4 days, before whiskers were plucked and immediately fixed by immersing, root first, in 10% formal saline for 30 minutes before storing in 4% saline at 4°C. Hair follicles from healthy volunteers were collected and processed as described above. The whisker and hair follicles underwent antigen retrieval with a citrate buffer (DAKO) prior to analysis. The cells, whisker and hair follicles were stained with anti-phospho-Thr246 PRAS40 (Upstate) and anti-PRAS40 (Cell Signalling Technology) antibodies (1:200 for cells; 1:50 for whisker and hair follicles), then visualized with 1:1000 AlexaFluor® 488 goat anti-rabbit IgG antibody (Invitrogen). Nuclei were counterstained with 1:10,000 TOPRO-3 (Invitrogen). The cells or follicles were mounted using Vectashield and images were visualized and captured using a Leica SP1 confocal laser scanning fluorescence microscope (Leica Microsystems). All images were taken with the same detector settings based on the respective vehicle-treated control sample. Optical magnification was 250, with an additional 2-fold software (digital) amplification, giving a total magnification of 500. For follicles, images were taken from the middle of the bulb along the z-axis and included the entire cross-section of the bulb. Fluorescence intensity in individual cells was quantified using the INCell Investigator Developer Toolbox v1.6 software (GE Healthcare). TOPRO-3 was used to identify all nuclei in the image. The areas around the boundary of the nuclei were then expanded to identify cytoplasmic regions. The nuclear and cytoplasmic segmentations were linked together, so that only cytoplasmic areas

of the image within cells with nuclei were quantified. The mean fluorescence intensity per cell was then reported from both the pThr246 PRAS40 and total PRAS40 images, respectively.

Statistics

Statistical significance was determined using unpaired t tests with GraphPad Prism 4 software.

Results

Discovery of a potent ATP-competitive inhibitor of AKT

CCT128930 was elaborated from an initial hit in a fragment screen using a structured-based design approach (12, 27). It consists of a pyrrolopyrimidine core, a 4-amino substituted piperidine and a 4-chlorobenzyl side chain (Figure 1A). CCT128930 is a potent ATP-competitive AKT inhibitor, which was initially screened at 10μmol/L against a panel of kinases representative of the human protein kinome. There was minimal cross-reactivity with 47 other kinases although inhibition of CHK2 and the AGC kinases p70S6K, PKA and Rock-II (<25% activity remaining) was observed (Supplementary figure 1). In view of the potential of ATP-competitive inhibitors to cross-react with the closely related AGC class of kinases, the IC_{50} of CCT128930 against selected AGC kinases was determined. CCT128930 was shown to be a potent and selective inhibitor of AKT2 (IC_{50} 6nM) with 28-fold selectivity over the closely related PKA kinase (IC_{50} 168nM) through the novel targeting of Met282 of AKT (Met173 of PKA-AKT chimera, Figure 1B, (12, 27)), as well as 20-fold selectivity over p70S6K (IC_{50} 120nM). These data indicate that CCT128930 is a potent and selective inhibitor of AKT.

CCT128930 activity in cells

The GI_{50} values of CCT128930 for growth inhibition (mean±SD) were 6.3 μM ± 2.2 (n=3) for U87MG human glioblastoma cells, 0.35 μM ± 0.11 (n=4) for LNCaP human prostate cancer cells, and 1.9 μM ± 0.80 (n=5) for PC3 human prostate cancer cells, all of which are *PTEN*-deficient human tumor cell lines (28).

Following one hour treatment of U87MG human glioblastoma cells with increasing concentrations of CCT128930, there was an initial induction of AKT phosphorylation at serine 473 up to 20 μM of CCT128930, followed by a decrease in phosphorylation at higher concentrations (Figure 2A). Total AKT signal stayed generally constant throughout the treatments. Decreased phosphorylation of AKT direct substrates or downstream targets was observed with increasing concentrations of CCT128930. Direct substrates of AKT (Ser9 GSK3β, pThr246 PRAS40 and pT24 FOXO1/p32 FOXO3a) were inhibited at ≥ 5 μM, and the downstream target, pSer235/236 S6RP, was inhibited at ≥ 10 μM CCT128930, with generally constant levels of the respective total proteins and GAPDH (Figure 2A). There were minimal effects of CCT128930 on pSer240/244 S6RP. Expression of the cell cycle protein cyclin D1 appeared to decrease at high concentrations (≥ 40 μM) of compound.

The effects of CCT128930 exposure over time on AKT activity were also investigated (Figure 2B). Treatment of U87MG human glioblastoma cells with 18.9 μM (3× GI_{50}) CCT128930 caused an increase in phosphorylation of pSer473 AKT after 30 minutes, which was sustained for 48 hours. Total AKT protein signal decreased gradually from 8 hours to 48 hours of treatment. There was a rapid and profound loss in pSer9 GSK3β phosphorylation starting from 30 minutes of CCT128930 treatment, which was sustained for at least 24 hours, before recovery at 48 hours. The corresponding total GSK3β protein signal remained relatively constant over this interval. CCT128930 induced a marked loss in phosphorylation of pThr246 PRAS40 from 30 minutes, which was sustained throughout 48 hours of treatment, while total PRAS40 signal remained unchanged. CCT128930 also caused a marked decrease in FOXO3a phosphorylation at threonine 32 (pThr32 FOXO3a) after a one hour exposure, while phosphorylation of Threonine 24 of FOXO1 (pThr24 FOXO1) and total FOXO1 remained generally constant. Total FOXO1 signal remained constant throughout treatment. There was a decrease in pSer235/236 S6RP signal at the earliest time point (30 minutes) with complete loss after 2 hours of treatment. In contrast, pSer240/244 S6RP signal decreased from 4 hours, and was abolished after 8 hours of CCT128930 treatment. Once again, the total S6RP protein signal remained relatively constant throughout treatment. The cell cycle marker cyclin D1 decreased after 8 hours of treatment, while there was induction of the cyclin-dependent kinase (CDK) inhibitor, p27, from 2 hours of CCT128930 treatment. It is important to note that apoptosis, as measured by PARP cleavage, was also shown to increase after CCT128930 treatment (Supplementary Figure 2).

The effects of one hour exposure to CCT128930 were also assessed in *PTEN*-null PC3 and LNCaP prostate cancer cell lines, HCT116 colorectal cancer cells and MCF7 human breast cancer cells (Figure 2C). As seen with *PTEN*-null U87MG human glioblastoma cells, these studies demonstrated an induction in pSer473 AKT, with constant levels of total AKT. Decreased phosphorylation of pSer9 GSK3β was observed in both the *PTEN*-null PC3 and LNCaP human prostate cancer cell lines, as well as the *PTEN*-wildtype, *PIK3CA*-mutated human colorectal cancer cells and MCF7 human breast cancer cells (28), while pSer240/244 S6RP decreased in all four cell lines, with total protein levels staying generally constant. Taken together, these molecular biomarker studies clearly show that CCT128930 inhibits AKT activity in cancer cells *in vitro*. There was no apparent correlation between the SRB assay GI_{50} and the IC_{50} for loss of phosphorylation on Ser9 GSK3β across the panel of 5 cell lines (data not shown), possibly due to the complexities of the survival pathways or small sample size.

Cell cycle effects of CCT128930

Inhibition of the PI3K pathway has been reported to cause a G1 cell cycle arrest (29–31) and therefore studies were performed to investigate the effects of CCT128930 concentration and exposure time on the cell cycle in U87MG human glioblastoma cells. In order to characterize the effects of CCT128930 on the cell cycle distribution in U87MG cells over time, a value of 3 × GI_{50} (18.9μM) was selected, since PI3K-AKT pathway inhibition had been observed at this concentration (Figure 2A). CCT128930 treatment of U87MG cells resulted in an increase in G0/G1 phase cells from 43.6% to 64.8% (Figure 3A and 3B) after 24 hours of treatment. This was associated with a decrease in S phase cells from 36.6% in

the DMSO control to 2.0% in the drug-treated cells. Cells in the corresponding G2/M phase increased from 17.8% in the DMSO control to 30.5% after 24 hours of treatment. Non-dividing cells in S phase (S') remained relatively constant throughout the treatment.

Cell cycle analysis of a concentration-response study of CCT128930 showed that 1 × GI_{50} caused an increase in G0/G1 phase cells from 46.4% in the DMSO control to 63.2% after 24 hours of treatment (Figure 3C). There was a corresponding decrease in S phase cells from 32.3% to 13.2% and a slight increase in G2/M cells from 16.7% to 18.9%. The number of cells in the S' phase was relatively constant. Comparable effects were seen at 3 × GI_{50}. This G1/S arrest occurred at CCT128930 concentrations ≥ 5μM consistent with inhibition of AKT activity (Supplementary Figure 3 and Figure 2A). Similar results were obtained after 48 hours of CCT128930 exposure (data not shown). These data show that CCT128930 caused a predominant G1 arrest, with a corresponding decrease in S phase in *PTEN*-null U87MG human glioblastoma cells in a time and drug concentration-dependent manner.

Pharmacokinetics of CCT128930

The pharmacokinetics of CCT128930 were determined to establish if therapeutically active drug concentrations could be established *in vivo*. The pharmacokinetics of CCT128930 after a single dose of 25 mg/kg are illustrated in Figure 4A and summarized in Supplementary Table 1. Following i.v. administration, CCT128930 reached a peak concentration of 6.4 μM in plasma and was eliminated with a relatively short half-life, high volume of distribution and rapid clearance, giving an $AUC_{0-\infty}$ of 4.6 μMh. Following i.p. administration, the peak plasma drug concentration was 4-fold lower and the plasma clearance was similar to that observed i.v.. The corresponding $AUC_{0-\infty}$ was 1.3 μMh, giving an i.p. bioavailability of 29%.

Oral CCT128930 administration gave a comparable pharmacokinetic profile to other routes, but the peak plasma concentration was only 0.43 μM, with a plasma clearance comparable to that observed iv suggesting no first pass metabolism (Supplementary Table 1). This resulted in a correspondingly low AUC and an oral bioavailability of only 8.5%. More importantly, following i.p. administration, peak tumor CCT128930 concentrations were 6-fold higher than the corresponding plasma value at 8 μM and there was evidence of drug retention, as shown by the 2-fold longer half-life and 6-fold slower apparent clearance. This resulted in much higher tumor drug exposure relative to plasma with an $AUC_{0-\infty}$ of 25.8 μMh. Tumor:plasma drug concentrations did not reach steady-state but varied from 4:1 at 30 minutes to 163:1 at 6 hours, confirming tissue drug retention. Assuming linear kinetics, these data supported the use of higher doses and repeat administration to achieve potentially therapeutic tumor drug concentrations *in vivo*.

Figure 4B shows that following CCT128930 administration at 50 mg/kg i.p. per day for 4 days, drug concentrations in U87MG human glioblastoma tumors were consistently much greater than the corresponding plasma concentrations with tumor:plasma ratios of 27:1 and 42:1 at 2 and 6 hours following the last dose, respectively. Moreover, U87MG tumor drug concentrations greatly exceeded the CCT128930 GI_{50} for at least 6 hours following the final dose and were consistently 5-fold higher than the concentrations required for *in vitro* biomarker modulation (Figure 2). Metabolism studies revealed that only 0.23% of an

administered dose (25 mg/kg i.p.) was recovered unaltered in urine after 24 hours (data not shown). The above results showed that pharmacologically active concentrations of CCT128930 were achieved in tumor tissue at well-tolerated doses.

Pharmacodynamic activity of CCT128930 *in vivo*

Having demonstrated concentration-dependent and time-dependent inhibition of numerous AKT biomarkers by CCT128930 *in vitro* and promising levels of tumor exposure *in vivo*, the pharmacodynamic effects of the compound were then evaluated in the same mice bearing U87MG human glioblastoma tumors, as used for the pharmacokinetic studies (Figure 4B). Figures 4C and D summarize the effects of CCT128930 treatment (50 mg/kg i.p. × 4 days) on several AKT biomarkers in U87MG xenografts harvested 2 and 6 hours following the last dose (see Figure 4B). CCT128930 caused a significant increase in Ser473 phosphorylation on AKT at both the 2 and 6 hour time points ($P<0.001$ and $P<0.01$, respectively), consistent with the biomarker results *in vitro* (compare Figure 3 to Figure 2). In addition, at both 2 and 6 hour time points, there were clear and significant decreases in the phosphorylation of Ser9 GSK3β ($P<0.001$ and $P<0.01$, respectively), Ser235/236 S6RP ($P<0.05$ and $P<0.01$, respectively) and Thr246 PRAS40 ($P<0.05$ and $P<0.05$, respectively), with the total forms of the protein remaining relatively constant (Figures 4C and D). These observations are consistent with inhibition of AKT activity by CCT128930 occurring in U87MG tumors *in vivo*.

Antitumor activity of CCT128930

Next, the antitumor activity of CCT128930 was evaluated in two molecularly relevant human tumor xenograft models. Figure 5A demonstrates that there was a marked antitumor effect of CCT128930 at 25 mg/kg i.p. (× 5 of 7 days) in established *PTEN*-null U87MG human glioblastoma xenografts, giving a treated:control (T/C) ratio on day 12 of 48%. There was no weight loss associated with this regime. Treatment of HER2-positive, *PIK3CA*-mutant BT474 human breast cancer xenografts (28) with CCT128930 (40 mg/kg bid × 5 of 7 days) also had a profound antitumor effect with complete growth arrest and a T/C ratio of 29% on day 22. This regimen was associated with minimal weight loss, with a nadir of only 94.8% of the initial body weight on day 15 of treatment. These results clearly demonstrate that CCT128930 has antitumor activity as a single agent in two human tumor xenograft models that are molecularly relevant with respect to PI3K pathway activation.

Development of a hair follicle pharmacodynamic biomarker assay for AKT activity

Finally, we developed a quantitative pharmacodynamic hair follicle PRAS40 biomarker assay with CCT128930 for use in clinical trials of AKT inhibitors. The effects of CCT128930 treatment on pThr246 and total PRAS40 were compared in *PTEN*-null U87MG human glioblastoma cells, whiskers obtained from BALB/c mice treated *in vivo* and hair follicles from human healthy volunteers. Initial studies showed that there was a significant decrease in pThr246 PRAS40 ($P<0.001$), while total PRAS40 stayed generally constant relative to the vehicle control following 24 hour of exposure to increasing concentrations of CCT128930 on U87MG cells (Supplementary Figure 4). Figure 6A and 6B show that there was a significant decrease ($P<0.001$) in pThr246 PRAS40 in whiskers plucked from mice treated with CCT128930 (50 mg/kg × 4 days i.p.) relative to controls, with minimal changes

in total PRAS40 expression. The influence of diurnal variation was not formally investigated, but no obvious fluctuations in the amount of baseline fluorescence levels (in the absence of AKT inhibitor) were observed. *Ex vivo* treatment of plucked, human healthy volunteer hair follicles incubated for 24 hours with increasing concentrations of CCT128930 showed that there was a significant decrease ($P<0.001$) in pThr246 PRAS40 signal at >3 × GI_{50} concentrations of CCT128930 (Figure 6C–6D), while total PRAS40 stayed generally constant. These results indicate that CCT128930 inhibits AKT activity in a surrogate normal tissue taken from both mouse and human and support this potential use of hair follicle measurements in clinical trials of AKT inhibitors.

Discussion

The PI3K-AKT signal transduction pathway is a critical driver of tumorigenesis, and a number of PI3K/AKT pathway inhibitors have now been disclosed with several recently entering the clinical arena (2, 9). In this report, we describe the preclinical pharmacology of CCT128930, a recently developed AKT inhibitor, which was discovered using fragment-based lead identification and structure-based design technologies and exhibited improved selectivity over PKA through the targeting of a specific amino acid residue Met282 of AKT (12). We have confirmed that CCT128930 is a potent and selective AKT inhibitor, which causes a predominant G_1/G_o cell cycle arrest, consistent with other reported specific inhibitors of the PI3K/AKT pathway. CCT128930 inhibited the phosphorylation of several AKT substrates including GSK3β, PRAS40 and FOXO1, as well as downstream targets S6RP and cyclin D1 in multiple cell lines *in vitro,* consistent with AKT inhibition. These effects were recapitulated *in vivo*. Antitumor activity was also observed in both *PTEN*-null U87MG human glioblastoma xenografts and HER2-positive, *PIK3CA*-mutant BT474 human breast cancer xenografts. Furthermore, a non-invasive and semi-quantitative immunofluorescent, biomarker assay for AKT inhibition was also developed using whisker follicles from mice treated with CCT128930 and human hair follicles treated *ex vivo* with this compound.

CCT128930 is a potent ATP-competitive AKT inhibitor, similar in mechanism to A-443654 (32) and GSK690693 (33), but distinct from the allosteric AKT inhibitor MK2206 (34), or perifosine (35), which interacts with the PIP3-binding pleckstrin homology domain of AKT. In the present study, CCT128930 caused an initial induction of phosphorylation on Ser473 of AKT at doses up to 20 μM in *PTEN*-null U87MG human glioblastoma cells, with eventual suppression at higher doses. Similar observations have been made with other ATP-competitive AKT inhibitors (33, 36). This has been hypothesized to be either directly due to inhibitor binding to the ATP binding site of AKT, or a result of compensatory but futile feedback loops of AKT pathway regulation (37, 38). Despite this initial induction of AKT phosphorylation, CCT128930 treatment clearly results in a dose and time-dependent decrease of phosphorylation of both direct and indirect targets of AKT in U87MG human glioblastoma cells (Figure 2A and 2B).

We have also demonstrated similar dose-dependent effects on AKT and downstream proteins in *PTEN*-null PC3 and LNCaP human prostate cancer cells, as well as cells harboring *PIK3CA* mutations, such as HCT116 human colorectal cancer cells and MCF7 human breast

cancer cells. Exposures as low as 5-10 μM for 1 hour were sufficient to markedly inhibit phosphorylation of GSK3β, S6RP, FOXO1 and PRAS40. Several of these proteins are involved in cell cycle and proliferation (GSK3β, cyclin D1 and p27), cell growth (PRAS40 and S6RP) and apoptosis (FOXO1), and this is consistent with the potent antiproliferative activity of CCT128930 *in vitro*. The loss of cyclin D1 and induction of the CDK inhibitor p27 are consistent with the cell cycle arrest at G1 and inhibition of the PI3K-AKT-mTOR signaling pathway (39–41). In addition we have observed induction of apoptosis, a known phenotype of AKT inhibition.

One of the key aims of this study was to identify and monitor appropriate biomarkers of AKT inhibition, in order to establish pharmacokinetic-pharmacodynamic relationships *in vitro* and *in vivo*, as well as to relate these findings to antitumor effects. Pharmacokinetic studies established that following i.p. administration, CCT128930 gave considerably higher and potentially therapeutic drug concentrations in tumor compared to plasma.

Pharmacodynamic biomarker and antitumor studies in *PTEN*-null U87MG human glioblastoma xenografts confirmed that AKT was inhibited by CCT128930 *in vivo* and that this was associated with a marked antitumor response at doses that were well tolerated. These pharmacodynamic studies were conducted to enable both target and pathway modulation to be monitored throughout the preclinical evaluation process, and also to enable the construction of a “pharmacologic audit trail” to ensure that the target inhibition correlated with antitumor activity (17, 42–44). Importantly, we have demonstrated that single agent CCT128930 suppressed downstream pharmacodynamic biomarkers in tumor tissues at doses that also inhibited the tumor growth of both *PTEN*-deficient U87MG human glioblastoma and HER2-positive, *PIK3CA*-mutant BT474 human breast cancer xenografts. These results also support the notion that the molecular characterization of tumors may be important for single agent AKT inhibitor activity.

In order to extrapolate this drug development approach to the clinic, we have developed a novel pharmacodynamic biomarker assay for use in plucked human hair follicles to assess drug effects in clinical trials. In contrast to previous studies, this assay is rapid, sensitive and quantitative. Importantly, it employs a more practical strategy utilizing immunofluorescence and confocal microscopy, in contrast to procedures involving paraffin embedding and immunohistochemistry used elsewhere (18, 19, 45). This approach may thus be easily incorporated into a clinical trial to serially monitor pharmacodynamic effects, in order to potentially guide key decision-making in drug development (17, 19, 42–44).

PRAS40 is a binding partner of mTOR, which mediates AKT signals to mTOR, and is implicated in oncogenesis, insulin resistance and neuronal cell death (46). PRAS40 was selected as a pharmacodynamic biomarker for CCT128930 inhibition of AKT because it is a direct substrate of AKT and hence its phosphorylation status would accurately reflect AKT modulation. Moreover, phosphorylation of PRAS40 was also acutely sensitive to inhibition by CCT128930 (Figure 2B). We first developed this strategy *in vitro* through the treatment of *PTEN*-null U87MG human glioblastoma cells with CCT128930, followed by the collection of whisker follicles from BALB/c mice treated with CCT128930 *in vivo*, and finally, *ex vivo* treatment of healthy volunteer hair follicles. Several limitations exist. Since

an intact hair follicle is required, it is not possible to stain for both phosphorylated and total forms of the biomarker on the same follicle simultaneously. Additional assay validation will be useful to define such parameters as lower limit of detection and to evaluate whether a statistically significant decrease from control or a specific percent decrease from control is an appropriate definition of effect.

This assay is also suitable for use with PI3K or allosteric AKT inhibitors, since the pharmacodynamic readout used is the downstream substrate PRAS40. In the future, this technique may potentially be developed further to include the analyses of multiple biomarkers per hair follicle through the use of antibodies directly labeled with distinct fluorophores. This hair follicle assay is currently being employed as a pharmacodynamic readout in the Phase I clinical trial of the allosteric AKT inhibitor MK2206 (20).

In conclusion, we have evaluated the pharmacological and therapeutic properties of the interesting and novel AKT inhibitor CCT128930. This is a leading example of the pyrrolopyrimidines series, with which we obtained selectivity for AKT over PKA by targeting a single amino acid difference, which we were the first to show (12, 13). We have demonstrated that CCT128930 suppresses the phosphorylation of downstream markers of AKT *in vitro* and *in vivo* and exhibits promising single agent antitumor activity in molecularly relevant human cancer models with appropriate pharmacokinetic and pharmacodynamic properties. We have also used this AKT inhibitor to develop a novel assay to quantify pharmacodynamic biomarker changes in a normal tissue following PI3K-AKT pathway blockade, and this assay may have broader applications in clinical trials of other related pathway inhibitors.

Supplementary Material

Refer to Web version on PubMed Central for supplementary material.

Abbreviations List

PI3K	phosphatidylinositol 3-kinase
mTOR	mammalian target of rapamycin
PH	pleckstrin homology
PIP_3	phosphatidylinositol (3,4,5)-trisphosphate
PDK1	phosphoinositide-dependent kinase 1
mTORC2	mammalian target of rapamycin complex 2
GSK3β	glycogen synthase kinase-3β
PRAS40	proline-rich AKT substrate 40
S6RP	S6 ribosomal protein
PTEN	phosphatase and tensin homolog on chromosome 10)

Europe PMC Funders Author Manuscripts

DMSO	dimethyl sulphoxide
BrdUrd	bromodeoxyuridine
PI	propidium iodide
s.c.	subcutaneously
i.p.	intraperitoneally
T/C	treated:control ratio
LY	LY294002
OA	Okadaic acid

References

1. Engelman JA. Targeting PI3K signalling in cancer: opportunities, challenges and limitations. Nat Rev Cancer. 2009; 9:550–62. [PubMed: 19629070]
2. Yap TA, Garrett MD, Walton MI, Raynaud F, de Bono JS, Workman P. Targeting the PI3K-AKT-mTOR pathway: progress, pitfalls, and promises. Curr Opin Pharmacol. 2008; 8:393–412. [PubMed: 18721898]
3. Andjelkovic M, Alessi DR, Meier R, et al. Role of translocation in the activation and function of protein kinase B. J Biol Chem. 1997; 272:31515–24. [PubMed: 9395488]
4. Alessi DR, James SR, Downes CP, et al. Characterization of a 3-phosphoinositide-dependent protein kinase which phosphorylates and activates protein kinase Balpha. Curr Biol. 1997; 7:261–9. [PubMed: 9094314]
5. Sarbassov DD, Guertin DA, Ali SM, Sabatini DM. Phosphorylation and regulation of Akt/PKB by the rictor-mTOR complex. Science. 2005; 307:1098–101. [PubMed: 15718470]
6. Frame S, Cohen P. GSK3 takes centre stage more than 20 years after its discovery. Biochemical Journal. 2001; 359:1–16. [PubMed: 11563964]
7. Brunet A, Bonni A, Zigmond MJ, et al. Akt promotes cell survival by phosphorylating and inhibiting a Forkhead transcription factor. Cell. 1999; 96:857–68. [PubMed: 10102273]
8. Mamane Y, Petroulakis E, LeBacquer O, Sonenberg N. mTOR, translation initiation and cancer. Oncogene. 2006; 25:6416–22. [PubMed: 17041626]
9. Courtney KD, Corcoran RB, Engelman JA. The PI3K pathway as drug target in human cancer. J Clin Oncol. 2010; 28:1075–83. [PubMed: 20085938]
10. Hudes G, Carducci M, Tomczak P, et al. Temsirolimus, interferon alfa, or both for advanced renal-cell carcinoma. N Engl J Med. 2007; 356:2271–81. [PubMed: 17538086]
11. Donald A, McHardy T, Rowlands MG, et al. Rapid evolution of 6-phenylpurine inhibitors of protein kinase B through structure-based design. J Med Chem. 2007; 50:2289–92. [PubMed: 17451235]
12. Caldwell JJ, Davies TG, Donald A, et al. Identification of 4-(4-aminopiperidin-1-yl)-7H-pyrrolo[2,3-d]pyrimidines as selective inhibitors of protein kinase B through fragment elaboration. J Med Chem. 2008; 51:2147–57. [PubMed: 18345609]
13. Davies TG, Verdonk ML, Graham B, et al. A structural comparison of inhibitor binding to PKB, PKA and PKA-PKB chimera. Journal of molecular biology. 2007; 367:882–94. [PubMed: 17275837]
14. Workman P, Collins I. Probing the probes: fitness factors for small molecule tools. Chem Biol. 2010; 17:561–77. [PubMed: 20609406]
15. Sarker D, Workman P. Pharmacodynamic biomarkers for molecular cancer therapeutics. Adv Cancer Res. 2007; 96:213–68. [PubMed: 17161682]

16. Tan DS, Thomas GV, Garrett MD, et al. Biomarker-driven early clinical trials in oncology: a paradigm shift in drug development. Cancer journal (Sudbury, Mass. 2009; 15:406–20.
17. Workman P. Auditing the pharmacological accounts for Hsp90 molecular chaperone inhibitors: unfolding the relationship between pharmacokinetics and pharmacodynamics. Mol Cancer Ther. 2003; 2:131–8. [PubMed: 12589030]
18. Camidge DR, Randall KR, Foster JR, et al. Plucked human hair as a tissue in which to assess pharmacodynamic end points during drug development studies. Br J Cancer. 2005; 92:1837–41. [PubMed: 15886708]
19. Williams R, Baker AF, Ihle NT, Winkler AR, Kirkpatrick L, Powis G. The skin and hair as surrogate tissues for measuring the target effect of inhibitors of phosphoinositide-3-kinase signaling. Cancer Chemother Pharmacol. 2006; 58:444–50. [PubMed: 16485116]
20. Yap, TA.; Papadopoulos, K.; Fearen, I., et al. First dose-finding study in cancer patients (pts) of a potent, selective, allosteric AKT inhibitor MK2206 (MK), incorporating pharmacodynamic (PD) and predictive biomarkers and showing profound pathway blockade. Proceedings of the 101st Annual Meeting of the American Association for Cancer Research; 2010 Apr 17-21; Washington, DC. Philadelphia (PA): AACR; 2010. Abstract nr 27
21. Skehan P, Storeng R, Scudiero D, et al. New colorimetric cytotoxicity assay for anticancer-drug screening. J Natl Cancer Inst. 1990; 82:1107–12. [PubMed: 2359136]
22. Walton MI, Eve PD, Hayes A, et al. The preclinical pharmacology and therapeutic activity of the novel CHK1 inhibitor SAR-020106. Mol Cancer Ther. 2010; 9:89–100. [PubMed: 20053762]
23. Wilson, GD. Analysis of DNA—measurements of cell kinetics by the bromodeoxyuridine/antibromodeoxyuridine method. Oxford: IRL Press; 1994.
24. Workman P, Aboagye EO, Balkwill F, et al. Guidelines for the welfare and use of animals in cancer research. Br J Cancer. 2010; 102:1555–77. [PubMed: 20502460]
25. Gowan SM, Hardcastle A, Hallsworth AE, et al. Application of meso scale technology for the measurement of phosphoproteins in human tumor xenografts. Assay Drug Dev Technol. 2007; 5:391–401. [PubMed: 17638539]
26. Bradford MM. A rapid and sensitive method for the quantitation of microgram quantities of protein utilizing the principle of protein-dye binding. Anal Biochem. 1976; 72:248–54. [PubMed: 942051]
27. McHardy T, Caldwell JJ, Cheung KM, et al. Discovery of 4-amino-1-(7H-pyrrolo[2,3-d]pyrimidin-4-yl)piperidine-4-carboxamides as selective, orally active inhibitors of protein kinase B (Akt). J Med Chem. 2010; 53:2239–49. [PubMed: 20151677]
28. Sanger Institute Cosmic database. http://www.sanger.ac.uk/genetics/CGP/cosmic/
29. Gao N, Zhang Z, Jiang BH, Shi X. Role of PI3K/AKT/mTOR signaling in the cell cycle progression of human prostate cancer. Biochem Biophys Res Commun. 2003; 310:1124–32. [PubMed: 14559232]
30. Casagrande F, Bacqueville D, Pillaire MJ, et al. G1 phase arrest by the phosphatidylinositol 3-kinase inhibitor LY 294002 is correlated to up-regulation of p27Kip1 and inhibition of G1 CDKs in choroidal melanoma cells. FEBS Lett. 1998; 422:385–90. [PubMed: 9498822]
31. Guillard S, Clarke PA, Te Poele R, et al. Molecular pharmacology of phosphatidylinositol 3-kinase inhibition in human glioma. Cell cycle (Georgetown, Tex. 2009; 8:443–53.
32. Luo Y, Shoemaker AR, Liu X, et al. Potent and selective inhibitors of Akt kinases slow the progress of tumors in vivo. Mol Cancer Ther. 2005; 4:977–86. [PubMed: 15956255]
33. Rhodes N, Heerding DA, Duckett DR, et al. Characterization of an Akt kinase inhibitor with potent pharmacodynamic and antitumor activity. Cancer Res. 2008; 68:2366–74. [PubMed: 18381444]
34. Lu, W.; Defeo-Jones, D.; Davis, LJ., et al. In vitro and in vivo antitumor activities of MK-2206, a new allosteric Akt inhibitor. Proceedings of the 100th Annual Meeting of the American Association for Cancer Research; 2009 Apr 18-22; San Diego, California (CA): AACR; 2009. Abstract nr 3714
35. Kondapaka SB, Singh SS, Dasmahapatra GP, Sausville EA, Roy KK. Perifosine, a novel alkylphospholipid, inhibits protein kinase B activation. Mol Cancer Ther. 2003; 2:1093–103. [PubMed: 14617782]

36. Han EK, Leverson JD, McGonigal T, et al. Akt inhibitor A-443654 induces rapid Akt Ser-473 phosphorylation independent of mTORC1 inhibition. Oncogene. 2007; 26:5655–61. [PubMed: 17334390]
37. Okuzumi T, Fiedler D, Zhang C, et al. Inhibitor hijacking of Akt activation. Nat Chem Biol. 2009; 5:484–93. [PubMed: 19465931]
38. Harrington LS, Findlay GM, Gray A, et al. The TSC1-2 tumor suppressor controls insulin-PI3K signaling via regulation of IRS proteins. The Journal of cell biology. 2004; 166:213–23. [PubMed: 15249583]
39. Gao N, Flynn DC, Zhang Z, et al. G1 cell cycle progression and the expression of G1 cyclins are regulated by PI3K/AKT/mTOR/p70S6K1 signaling in human ovarian cancer cells. Am J Physiol Cell Physiol. 2004; 287:C281–91. [PubMed: 15028555]
40. Raynaud FI, Eccles S, Clarke PA, et al. Pharmacologic characterization of a potent inhibitor of class I phosphatidylinositide 3-kinases. Cancer Res. 2007; 67:5840–50. [PubMed: 17575152]
41. Fan QW, Knight ZA, Goldenberg DD, et al. A dual PI3 kinase/mTOR inhibitor reveals emergent efficacy in glioma. Cancer Cell. 2006; 9:341–9. [PubMed: 16697955]
42. Workman P. Challenges of PK/PD measurements in modern drug development. Eur J Cancer. 2002; 38:2189–93. [PubMed: 12387843]
43. Workman P. How much gets there and what does it do?: The need for better pharmacokinetic and pharmacodynamic endpoints in contemporary drug discovery and development. Current pharmaceutical design. 2003; 9:891–902. [PubMed: 12678873]
44. Yap TA, Sandhu SK, Workman P, de Bono JS. Envisioning the future of early anticancer drug development. Nat Rev Cancer. 2010; 10:514–23. [PubMed: 20535131]
45. Camidge DR, Pemberton M, Growcott J, et al. A phase I pharmacodynamic study of the effects of the cyclin-dependent kinase-inhibitor AZD5438 on cell cycle markers within the buccal mucosa, plucked scalp hairs and peripheral blood mononucleocytes of healthy male volunteers. Cancer Chemother Pharmacol. 2007; 60:479–88. [PubMed: 17143601]
46. Vander Haar E, Lee SI, Bandhakavi S, Griffin TJ, Kim DH. Insulin signalling to mTOR mediated by the Akt/PKB substrate PRAS40. Nature cell biology. 2007; 9:316–23. [PubMed: 17277771]

Europe PMC Funders Author Manuscripts

Europe PMC Funders Author Manuscripts

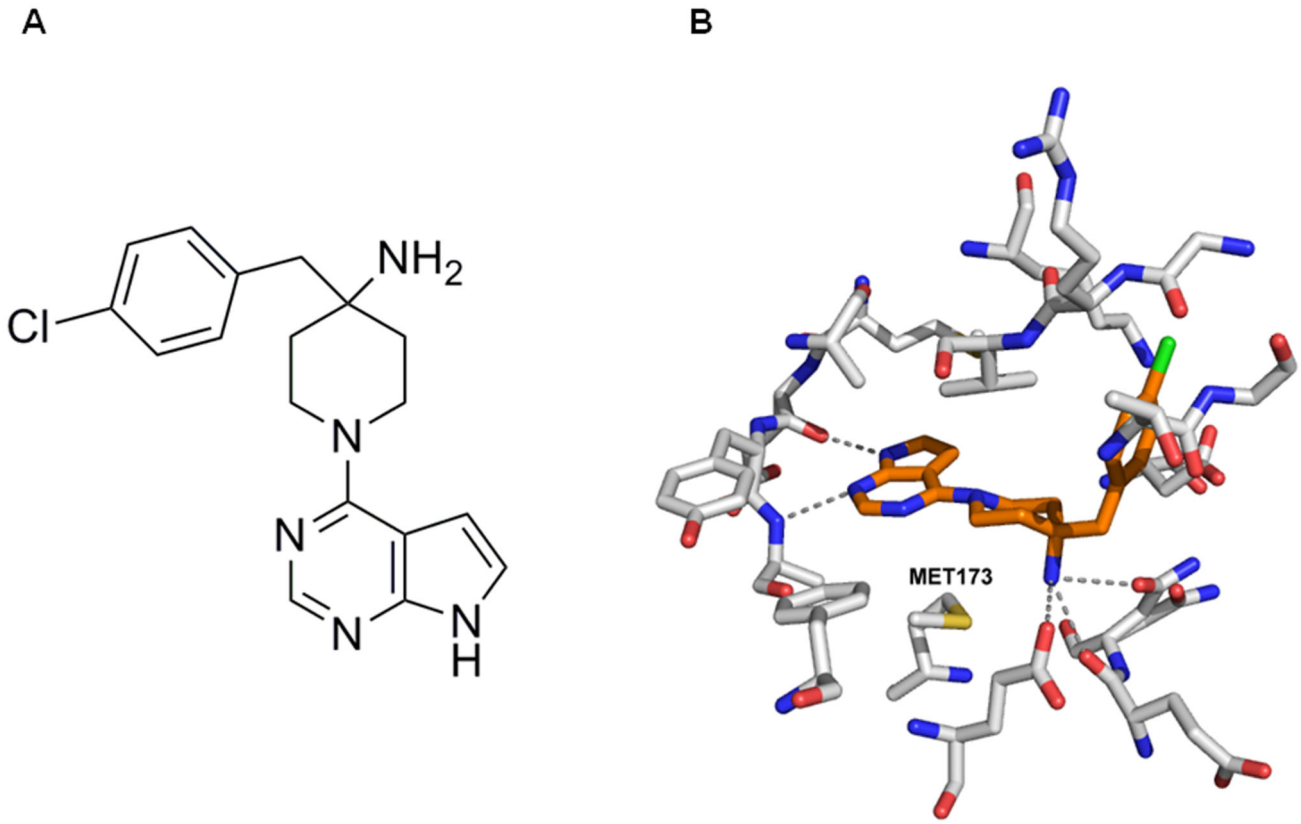

Figure 1. Chemical structure of CCT128930 and crystal structure of CCT128930 bound to a chimeric PKA-AKT protein.

A Chemical structure of CCT128930 (4-(4-chlorobenzyl)-1-(7H-pyrrolo[2,3-d]pyrimidin-4-yl)piperidin-4-amine)

B X-ray crystal structure of CCT128930 bound to PKA-AKT chimeric protein (PDB code 2V06; (12)). The inhibitor (amber) and key residues in the ATP-binding site (grey) are shown with hydrogen-bonding interactions indicated (dashed lines). The residue targeted by CCT128930 to give selective inhibition of AKT over PKA is highlighted (Met173 in PKA-AKT chimera, equivalent to Met282 in AKT) (12, 13).

Europe PMC Funders Author Manuscripts

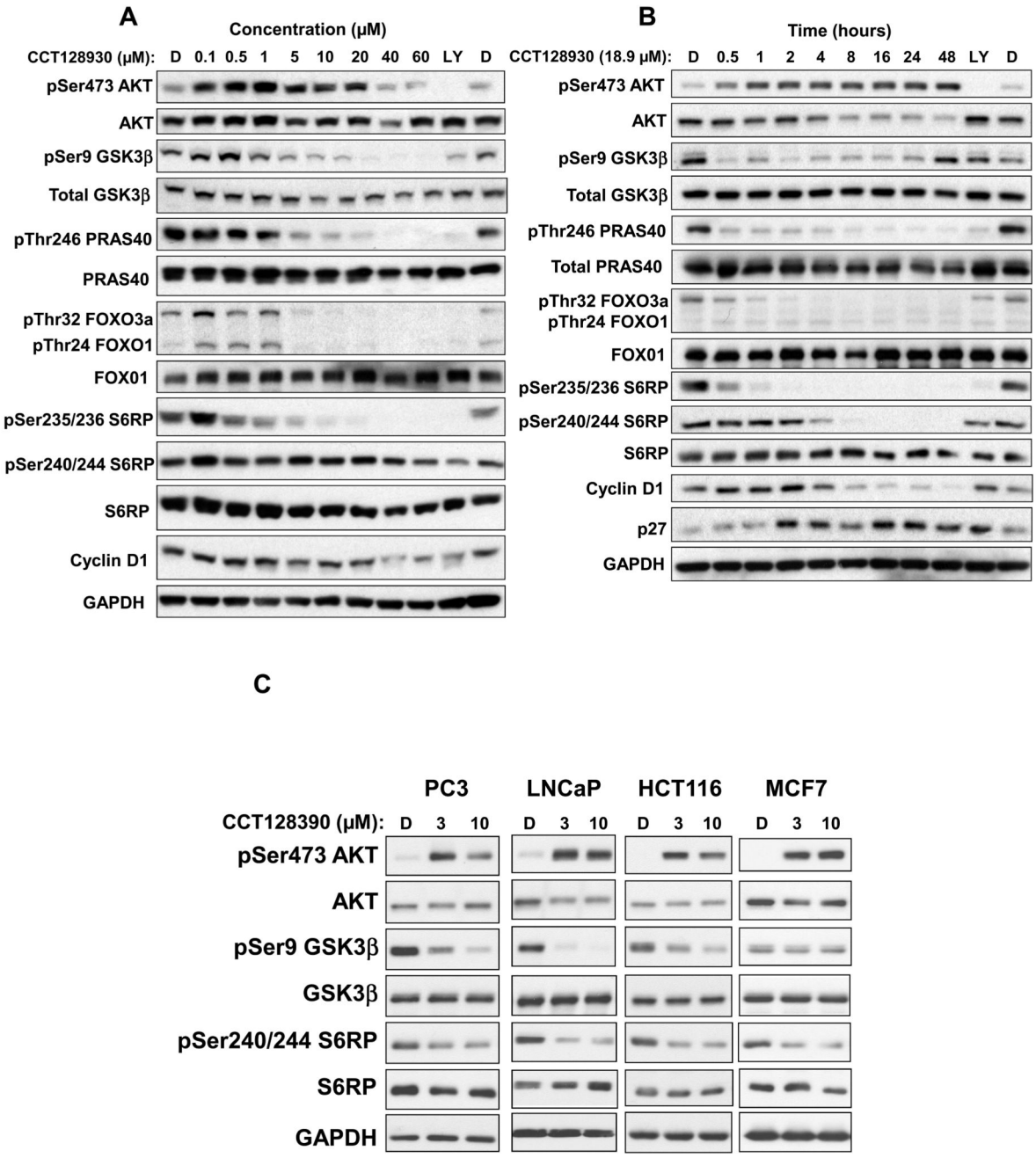

Figure 2. Effect of CCT128930 exposure on expression of AKT biomarkers and cell cycle proteins in a panel of human tumor cell lines.

A, *PTEN*-null U87MG human glioblastoma cells were exposed to different concentrations of CCT128930 for 1 hour. **B,** U87MG human glioblastoma cells were treated with a fixed concentration of CCT128930 (3 × GI_{50} (18.9μM)) and samples taken at intervals up to 48 hours following initial CCT128930 treatment. **C,** Four additional human cancer cell lines was exposed to a fixed concentration of CCT128930 for 1 hour (3 or 10 μM). Protein expression was measured by immunoblotting using GAPDH as a loading control. D is

DMSO treated control. LY is a positive control (LY294002 30μM for 1 hour). Similar results were obtained in repeat experiments.

Europe PMC Funders Author Manuscripts

Europe PMC Funders Author Manuscripts

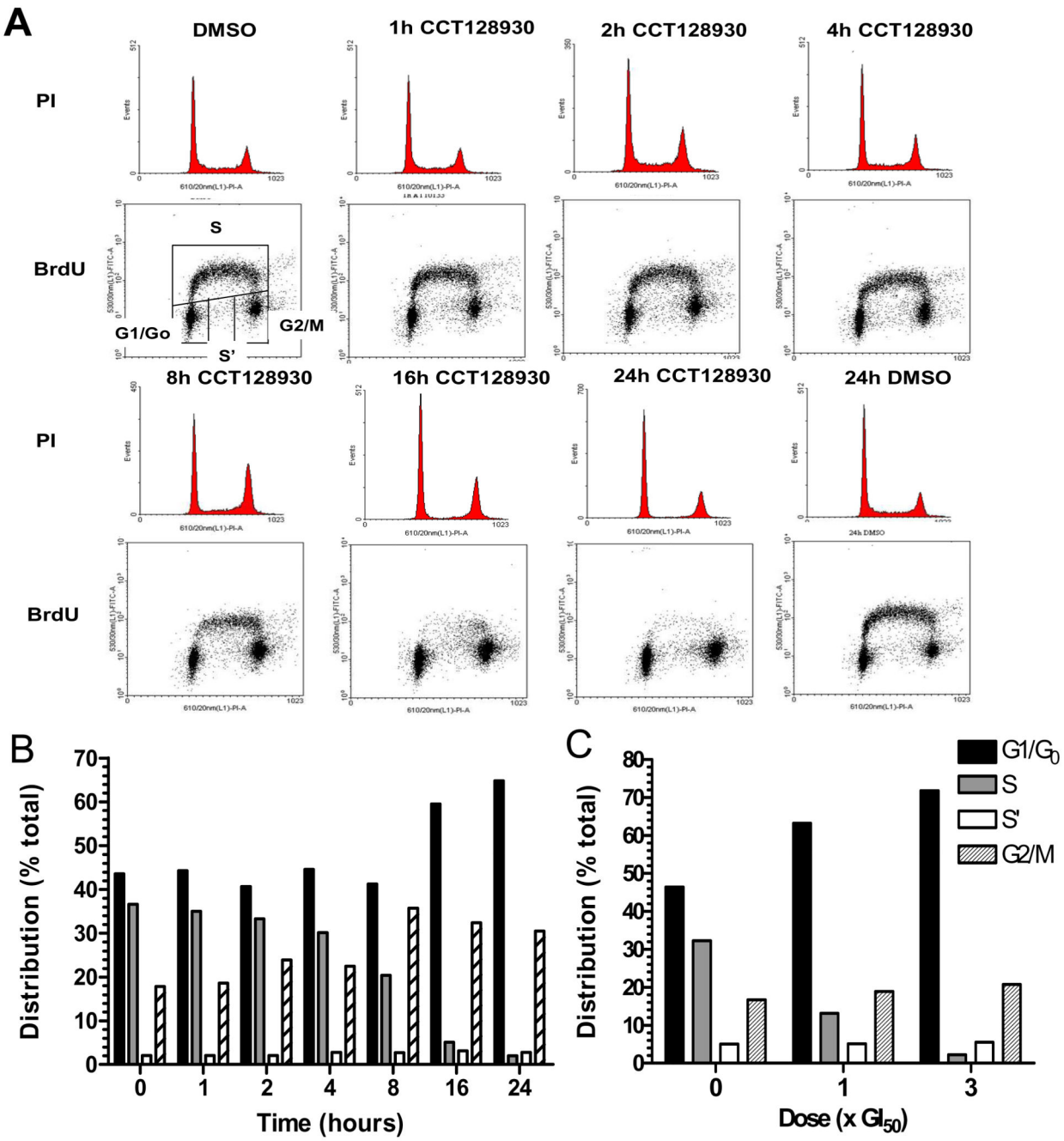

Figure 3. Cell cycle response of *PTEN*-null U87MG human glioblastoma cells to CCT128930.

A, Effect of a fixed concentration of CCT128930 ($3 \times GI_{50}$) on cell cycle distribution in *PTEN*-null U87MG human glioblastoma cells over a 24-hour time period. Histograms represent cell cycle distribution. Dot plots represent DNA synthesis in individual cells as measured by BrdUrd labeling and DNA content as measured by PI staining. Cell cycle distribution was quantified by BrdUrd analysis as described in Materials and Methods. **B,** Quantification of the effects described in A. **C,** Quantification of the effects of different

concentrations of CCT128930 on cell cycle distribution of U87MG human glioblastoma cells at 24 hours. Similar results were obtained in a repeat experiment.

Europe PMC Funders Author Manuscripts

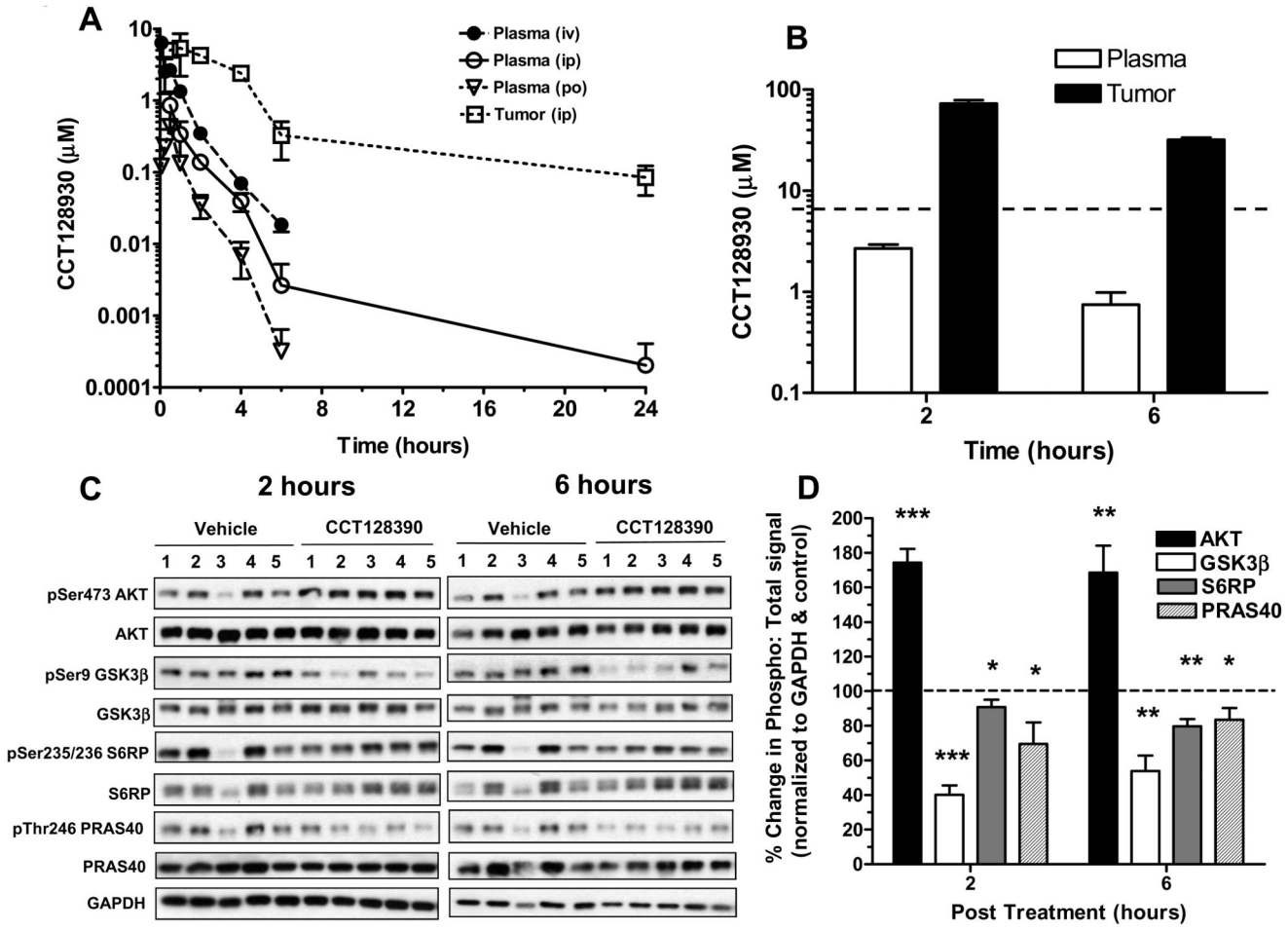

Figure 4. Pharmacokinetic behavior and pharmacodynamic effects of CCT128930 *in vivo*.

A, Pharmacokinetic profiles of CCT128930 in plasma and *PIK3CA*-mutant HCT116 human colon tumor xenograft from mice administered a single dose (25 mg/kg) either i.v. (•), i.p. (plasma ○ ; tumor □) or p.o. (∇). Data are mean ± SE with 3 to 5 mice per time point. **B,** Concentrations of CCT128930 measured in plasma (clear bars) and *PTEN*-null U87MG human glioblastoma xenografts grown s.c. in the flanks of CrTacNCr-*Fox1nu* mice (black bars), 2 hours and 6 hours following the last dose of 4 consecutive daily doses of 50 mg/kg i.p. The broken line indicates 96-hour GI_{50} value for CCT128930 in U87MG human glioblastoma cells *in vitro*. Bars represent mean ± SE for 3 determinations. **C,** AKT-dependent biomarker changes measured in the tumors taken from B. Protein expression was measured by immunoblotting. GAPDH was used as a loading control. **D,** Quantification of phosphoprotein changes relative to total protein expression after normalization to GAPDH for the immunoblots shown in C. Bars represent mean ± SE for 3-5 determinations. ■ pSer473 AKT: total AKT ratio; □ pSer9 GSK3β: total GSK3β ratio; ▒ pSer235/236 S6RP: total S6RP ratio; and ▨ pThr246 PRAS40: total PRAS40 ratio. Horizontal dashed line represents these ratios in controls = 1.0 (100%). Statistics: * P<0.05, ** P<0.01 and *** P<0.001 significantly different from vehicle treatment.

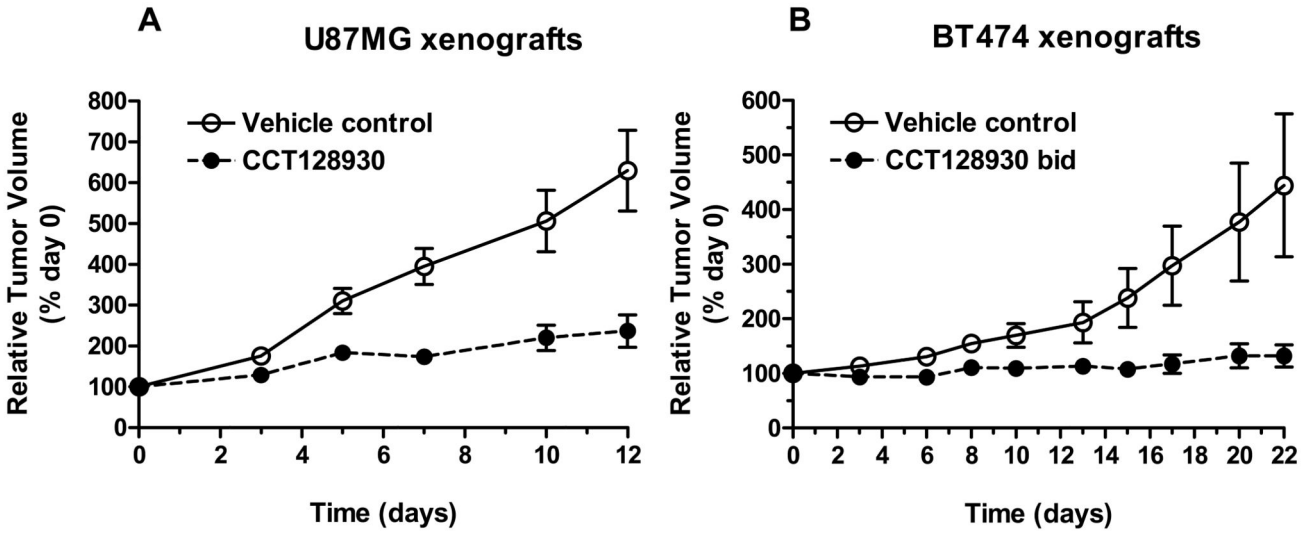

Figure 5. Antitumor activity of CCT128930 in human tumor xenografts.

A, Antitumor activity of CCT128930 (25 mg/kg i.p. qd × 5 of 7 days) in established *PTEN*-null U87MG human glioblastoma xenografts. ○ Vehicle control, ● CCT128930. **B,** Antitumor effects of CCT128930 (40 mg/kg i.p. bid × 5 of 7 days) in human HER2-positive, *PIK3CA*-mutant BT474 breast cancer xenografts. ○ Vehicle control, ● CCT128930. Values are mean ± SE for 5 to 8 mice per time point. Tumor size was assessed as described in the Material and Methods.

Europe PMC Funders Author Manuscripts

Europe PMC Funders Author Manuscripts

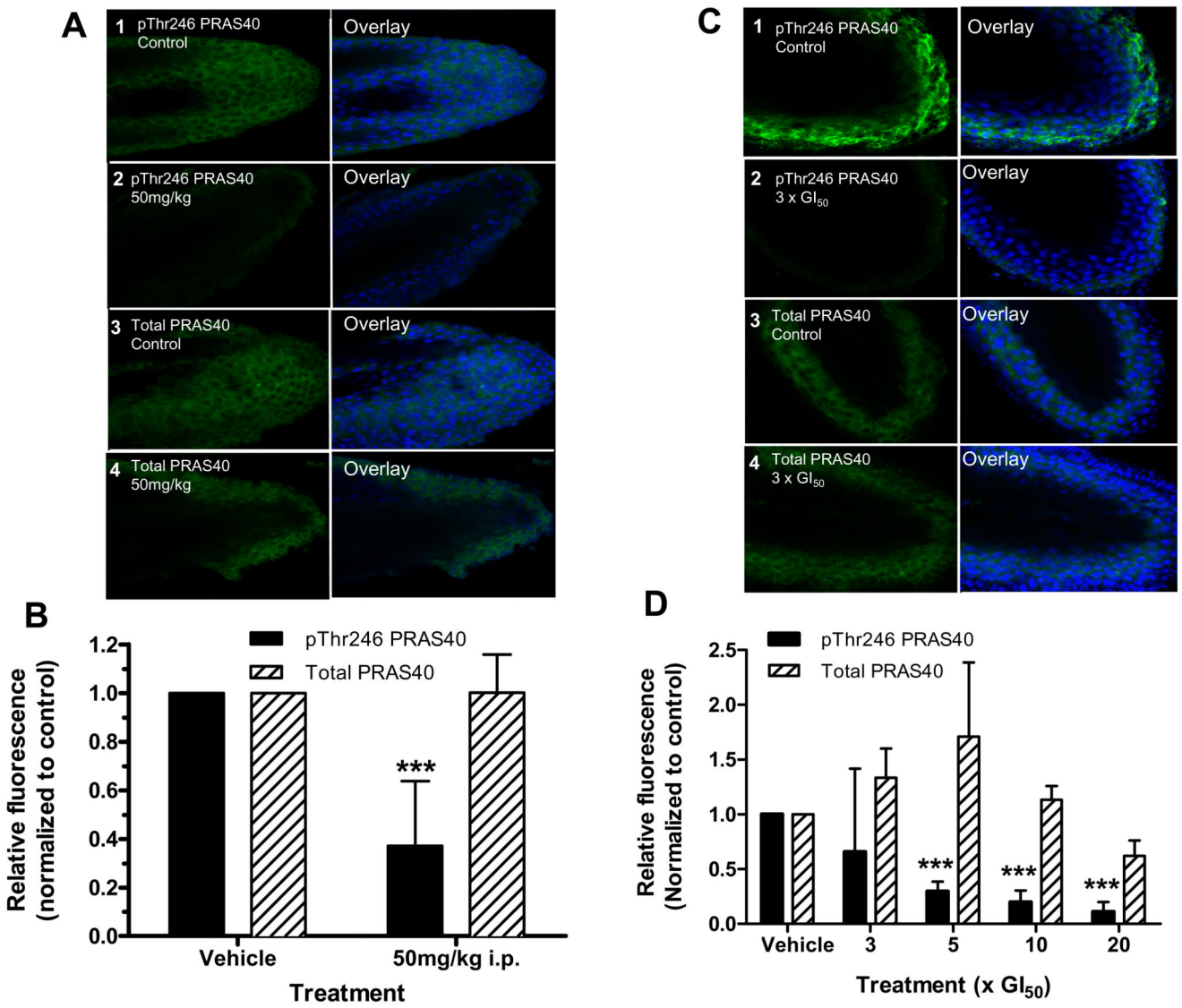

Figure 6. Effects of CCT128930 treatment on phosphorylated PRAS40 expression in mouse and human hair follicles.

A, Expression of pThr246 PRAS40 and total PRAS40 in whisker follicles from BALB/c mice taken 2 hours after the last of four daily doses of CCT128930 (50 mg/kg i.p.). Panel **1** shows control pThr246 PRAS40 expression from vehicle-treated mice, panel **2** shows pThr246 PRAS40 expression from CCT128930-treated mice, panels **3** and **4** show the corresponding total PRAS40 expression from vehicle and CCT128930-treated mice, respectively. The left hand panel shows immunofluorescent protein staining (green) and the right hand panel TOPRO-3 nuclear DNA staining (blue). Magnification was 500. Similar results were obtained in repeat experiments. **B,** Quantification of data shown in A. Results are mean ± SE for 15 determinations. Statistics: *** P<0.001 significantly different from vehicle-treated samples (expression normalized to 1). **C,** Expression of pThr246 PRAS40 in normal human hair follicles following 24 hours exposure to 3 × GI_{50} CCT128390 *ex vivo*. Panel **1** shows pThr246 PRAS40 expression in vehicle-treated hairs. Panel **2** shows pThr246

PRAS40 expression in hairs treated with 3 × GI_{50} CCT128390. Panels **3** and **4** show the corresponding total PRAS40 expression from vehicle and CCT128930-treated hairs, respectively. Magnification was 500. **D,** Quantification of pThr246 PRAS40 changes relative to control in normal human hairs treated with different concentrations of CCT128390 for 24 hours *ex vivo*. The GI_{50} value employed was 6.3μM as determined in the *PTEN*-null U87MG glioblastoma cell line. Values are mean ± SE for 4 values determined in 4 independent experiments. Statistics: *** P<0.001 significantly different from control samples (expression normalized to 1).

Europe PMC Funders Author Manuscripts